ELSEVIER

International Journal of Refractory Metals & Hard Materials 17 (1999) 431–435

International Journal of
REFRACTORY METALS
& HARD MATERIALS

Grain subdivision and recrystallization in oligocrystalline tantalum during cold swaging and subsequent annealing

Hugo R.Z. Sandim [a,*,1], Angelo F. Padilha [b], Valerie Randle [c], Wolfgang Blum [a]

[a] *Institut für Werkstoffwissenschaften, Universität Erlangen-Nürnberg, D-91058 Erlangen, Germany*
[b] *Department of Metallurgical and Materials Engineering, University of São Paulo, 05508-900 São Paulo-SP, Brazil*
[c] *Department of Materials Engineering, University of Wales Swansea, Swansea SA2 8PP, UK*

Received 16 September 1999; accepted 21 October 1999

Abstract

A coarse-grained ingot of high-purity tantalum was deformed by swaging at room temperature to a strain of 1.28. During annealing at 900°C for 30 min two neighboring grains were observed to behave quite differently. Electron backscattering diffraction (EBSD) results show noticeable differences in terms of the misorientations developed in both grains. The grain developing larger misorientations recrystallized much more readily than the other. The result is interpreted in terms of the differences in grain subdivision into strongly misoriented regions.

Keywords: Tantalum; Cold swaging; Recovery; Recrystallization and misorientation

1. Introduction

Tantalum is widely used in chemical, electronic and aerospace applications because of its unique properties including high corrosion resistance, a high melting point ($T_m = 3269$ K) and high thermal and electrical conductivities [1]. Electron beam melting is a convenient technique to obtain tantalum in high purity. It leads to oligocrystalline ingots consisting of coarse columnar grains aligned parallel to the longitudinal axis.

These ingots can be further processed by cold swaging to large strains and subsequent annealing. Cold deformation leads to subdivision of the grains into misoriented regions. Such grain subdivision into subgrains is a well-known phenomenon also in deformation at high homologous temperatures (hot deformation and creep). However, there are distinct differences between hot and cold deformation. With decreasing temperature the fraction of subgrain boundaries which reach misorientations above the approximate 15°-limit of low angle boundaries increases appreciably. With increasing strain these boundaries become parallel to the direction of elongation leading to a subdivision of the grains into strongly misoriented lamellae. This has also been observed for tantalum [2,3]. The details of grain subdivision are important for the recrystallization behavior of the material during annealing of the deformed structure.

In this work the progress of recrystallization during annealing of cold swaged tantalum has been studied in two neighboring grains. Due to the low homologous temperature $T/T_m = 0.35$ of annealing, the early stages of recrystallization could be seen. It will be shown that the recrystallization behaviors of the two grains differ significantly. This behavior is related to the differences in subdivision of the two grains.

2. Experimental

A high-purity coarse-grained ingot was obtained by means of double electron beam melting of tantalum reverts. Average dimensions of these coarse columnar grains were about 40 mm length and 10 mm width. The tantalum ingot was deformed by swaging at room temperature to a true strain $\varepsilon = 1.28$ (corresponding to a reduction in cross-section by 72%) without intermediary annealing. The temperature rise during swaging was limited to about 100°C. After swaging, the bar was vacuum annealed at 900°C for 30 min. Further details are reported elsewhere [4]. Metallographic preparation

* Corresponding author.
[1] On leave from Department of Materials Engineering, FAENQUIL, P.O. Box 116, Lorena-SP, 12600-000, Brazil.

0263-4368/99/$ - see front matter
PII: S0263-4368(99)00035-9

in longitudinal sections was carried out by means of conventional techniques including intermediary chemical polishing (in a solution $1HF:1HNO_3:2.5H_2SO_4$ held at 0°C) to remove the deformation effects caused by grinding. The microstructure was investigated by means of light optical microscopy (LOM) using the interference contrast technique. Channelling contrast images were obtained from a JEOL JSM 6400 scanning electron microscope (SEM) operating in the backscatter (BSE) mode at 10 kV. Electron backscattering diffraction (EBSD) patterns were recorded with an Oxford Instruments OPAL EBSD system interfaced to a JEOL 6100 SEM operating at 20 kV. From each of these patterns the local orientation was obtained by automatic indexing after suitable image processing. Pole figures and misorientation distribution are based on 512 orientation measurements taken in an area of about 300 μm × 700 μm at the points of a square grid with a distance of 22 μm between the neighboring sampling points.

3. Results

3.1. Microstructure

Fig. 1 shows LOM-pictures of sections of two neighboring grains 1 and 2 of the oligocrystalline tantalum ingot after swaging and annealing. We will call them old grains in contrast to the new grains which have formed in the course of recrystallization. A–D are the places where detailed microstructural and microtextural information was acquired. Fig. 2 presents region A and its surroundings in greater detail. Banded structures in the old grains are interpreted as coarse slip bands. This interpretation is confirmed by the comparison of the LOM- and SEM-micrographs of region D (Fig. 3). In the SEM picture the subgrain structure of the recovered material becomes visible, diminishing the contrast of the slip bands. Nevertheless the slip bands remain visible in SEM by their sharper contrast, indicating larger subgrain misorientations and their more elongated shape.

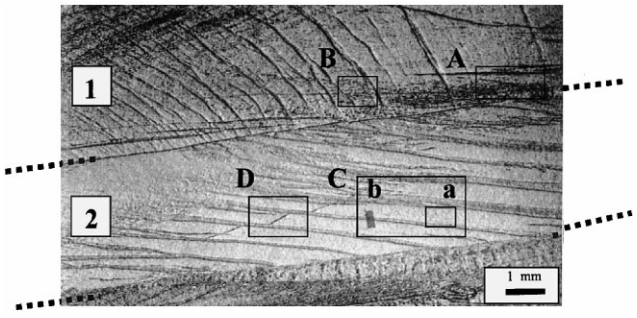

Fig. 1. Longitudinal view of tantalum deformed by cold swaging to $\varepsilon = 1.28$ and annealed at 900°C for 30 min (LOM).

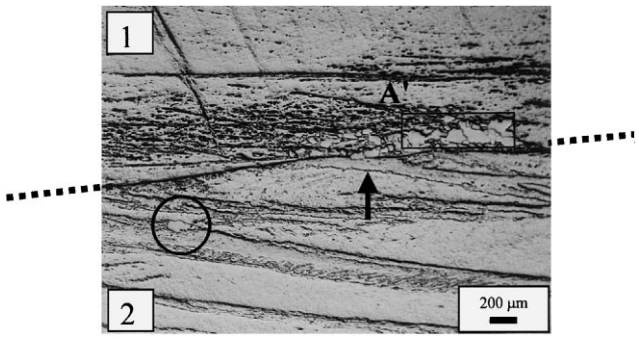

Fig. 2. Detailed view showing preferential recrystallization near grain boundary in grain 1 and grain boundary nucleation (marked by an arrow). A′ marks the region where EBSD was performed. Circle marks an isolated recrystallized grain. Dashed lines mark the position of the original grain boundaries.

A close inspection of Fig. 2 shows large recrystallized grains at and near region A. Fig. 4a confirms this observation by SEM. The statically recrystallized grains are characterized by the homogeneity of their appearance indicating that they are completely free from substructure. To the left of A the new grains become smaller (Figs. 2 and 4b). Many of the black spots in Figs. 1 and 2 correspond to very small recrystallized grains.

One finds these spots throughout grain 1, e.g. also in the upper left of Fig. 2. The recrystallized areal fraction (f_{RX}) of grain 1 is about 0.2. In grain 2, on the other hand, the appearance of recrystallized grains is a rare exception so that the recrystallized fraction is close to 0; a single new grain is marked by a circle. Correspondingly, the typical SEM-view of grain 2 shows a subgrain structure without recrystallized grains as shown in Figs. 3 and 4c.

3.2. Microtexture

Clear EBSD-patterns could be recorded in the recrystallized grains as well as in the recovered subgrains so that the local orientation could be determined. Fig. 5 shows representative {1 1 0}-pole figures taken in regions A and B of grain 1 and region C of grain 2 (these regions are indicated in Fig. 1).

Grain 1: In the sampling area corresponding to Fig. 5b the recrystallized fraction was rather small, about 0.2. This means that the pole figure comes mainly from the subgrain structure of region B in grain 1. Here the final ⟨1 1 0⟩-orientation has not yet been fully reached, as the ⟨1 1 0⟩-direction still deviates by about 15° from the longitudinal direction. The orientation difference between grains 1 and 2 is obvious from comparison of Fig. 5b and c. In the sampling area corresponding to Fig. 5a (region A′ in Fig. 2) the recrystallized fraction was high, about 0.9. Thus the pole Fig. 5a represents the recrystallized grains. Comparison with Fig. 5b shows that the

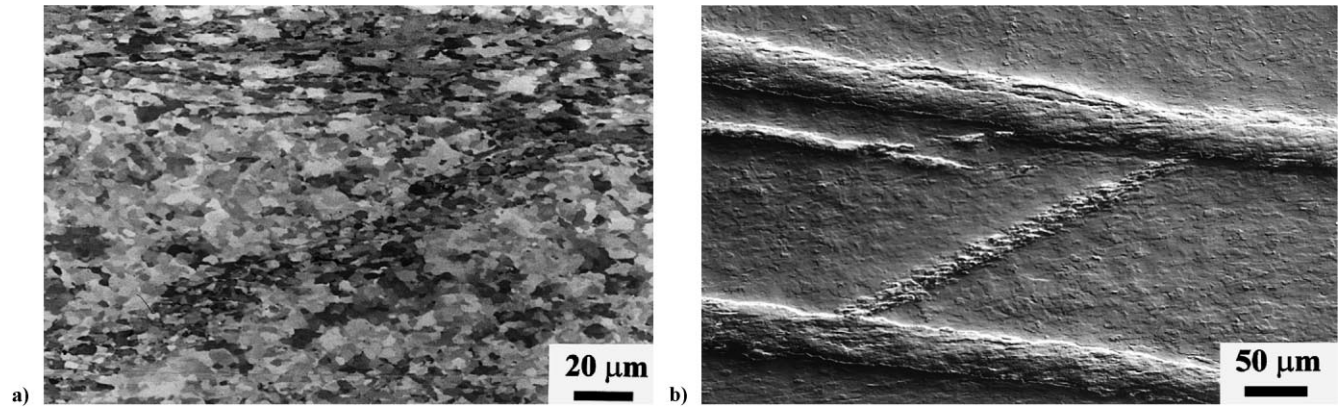

Fig. 3. Substructure in region D of grain 2 (SEM-BSE): (a) bands exhibiting localized deformation in the upper part and in the diagonal; (b) same region observed at LOM.

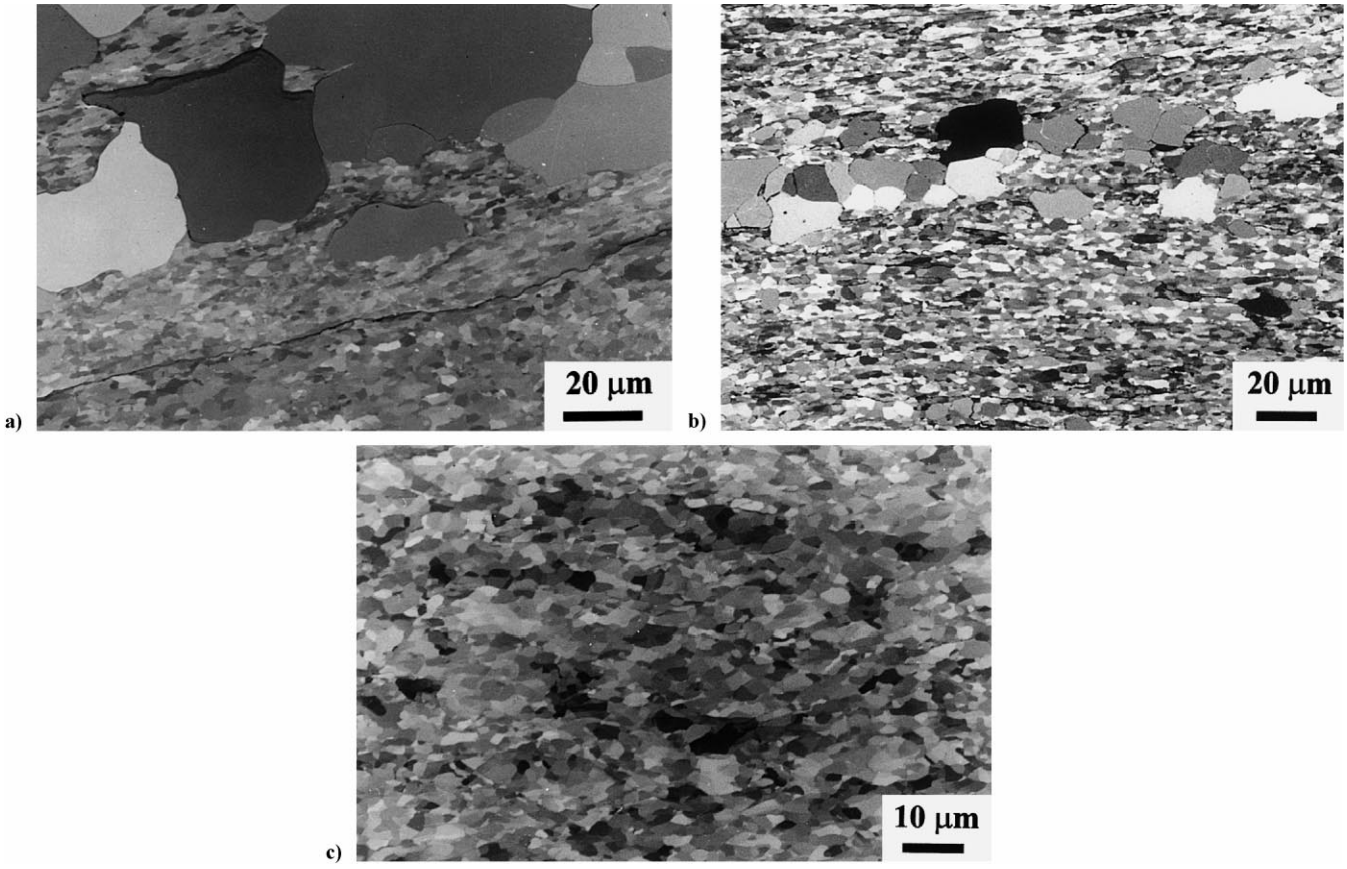

Fig. 4. Longitudinal section of Ta swaged to $\varepsilon = 1.28$ and annealed at 900°C for 30 min showing the microstructure (SEM-BSE) in: (a) region A; (b) region B; (c) region C (corresponding to **a** in Fig. 1).

orientation of the recrystallized grains is not far from that of the subgranular matrix indicating that subgrains acted as nuclei.

Grain 2: As there are no recrystallized grains in region C, Fig. 5c corresponds to the recovered subgrain structure of grain 2. The ⟨1 1 0⟩-direction is closely parallel to the longitudinal direction. Such orientation is expected from the ⟨1 1 0⟩-fiber texture produced by wire drawing of bcc metals, as wire drawing and swaging both involve axisymmetric elongation. In Fig. 5c one notices a certain orientation spread corresponding to the rotation around the ⟨1 1 0⟩-axis. This spread is not surprising because the

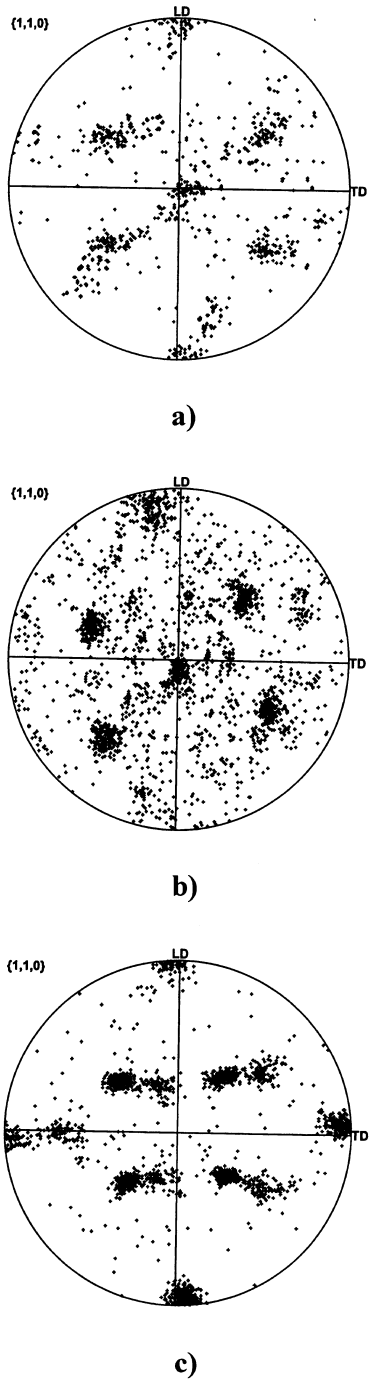

Fig. 5. {1 1 0}-pole figures from EBSD measurements in: (a) region A ($f_{RX,\ EBSD} \approx 0.9$); (b) region B ($f_{RX,\ EBSD} \approx 0.2$); (c) region C ($f_{RX,\ EBSD} = 0$).

area where the pole figure was sampled (see the dark field marked with **b** in Fig. 1) included a coarse slip band, which due to the difference in glide activity inside and outside the slip band is misoriented relative to its surroundings.

The orientation measurements were used to determine the misorientations Ψ between the sampling points

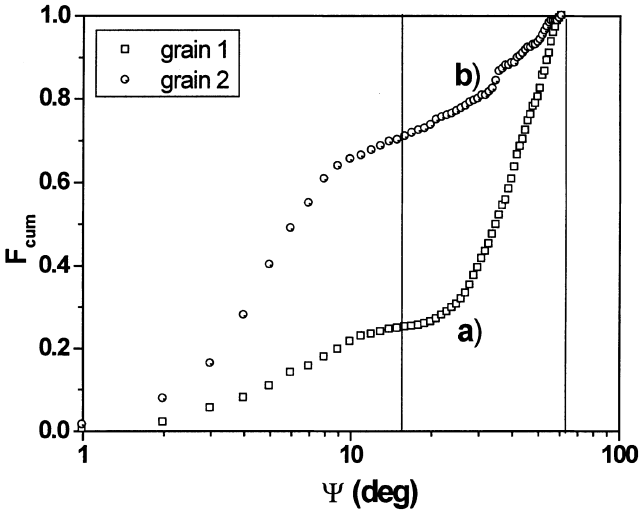

Fig. 6. Cumulative distribution of misorientations (Ψ) measured in longitudinal section in regions: (a) B (grain 1) and (b) C (grain 2) from EBSD measurements.

(Fig. 6). The distance between the sampling points (22 μm) is larger than the estimated size (4 μm) of the subgrains derived from SEM pictures. As only part of the boundaries shows up in SEM, the true subgrain size is smaller than 4 μm. Thus Ψ represents the accumulated misorientation of an ensemble of more than four neighboring subgrain boundaries.

In region C of grain 2, 70% of the measured Ψ-values are below 15°. Most of the 30% of Ψ-values exceeding 15° can be associated with the orientation gradient due to the coarse slip band traversing region C (see Fig. 1). This means that the fraction of boundaries with large angle character (>15°) is distinctly less than 30%.

In region B of grain 1, 75% of the measured Ψ-values lie above 15°. Thus the orientation spread is much larger than in grain 2. The sampling area in region B contains an areal fraction of 20% of recrystallized grains. The size of the new grains in this region is about 15 μm. This is smaller than the distance of the sampling points. Therefore 20% of the measured Ψ are due to the recrystallized grains. Assuming that these Ψ-values lie predominantly in the range above 15°, the fraction of Ψ-values above 15° in the subgranular matrix of grain 1 is about 44%.

4. Discussion

The two grains investigated in this work in the initial phase of recrystallization after cold swaging behave quite differently. While about 20% of grain 1 have recrystallized, recrystallization is virtually absent in grain 2. This difference must have its origin in the deformed structure. Due to the relatively large strain, both grains

have similar orientation relative to the longitudinal direction corresponding to the expected deformation texture.

Static recovery during annealing has transformed the dislocation structure present after cold swaging into a subgrain structure with subgrain sizes below 4 μm. The major difference in the recovered subgrain structures of the two grains lies in the magnitude of the orientation differences indicating that the misorientations of the subgrain boundaries are much larger in grain 1 than in grain 2.

It is known that grains with different initial orientation behave differently with regard to subdivision into subgrains. Theyssier et al. [5] reported that favorably oriented grains of aluminum deform in a stable manner during plane strain compression with the result that the boundary misorientations remain relatively small. Strong differences with respect to the recrystallization behavior were observed in coarse-grained high-purity aluminum deformed by cold rolling [6,7]. While some of the deformed grains exhibited fully recrystallization, some displayed only recovery after annealing. The progress of recrystallization is retarded in stably deforming grains in some bcc metals and alloys [8,9]. Similarly, Vandermeer and Snyder [10] found great differences between differently oriented single crystals of tantalum: some grains recrystallized easily, whereas in other presumably stably deforming single crystals recrystallization was strongly suppressed. Sandim et al. [3] showed that grain subdivision differed from grain to grain in coarse-grained tantalum during cold swaging; while most grains developed a lamellar structure, such structure of strongly misoriented lamellae was missing in a significant minority of grains.

The difference in grain subdivision gives a clue to interpret the present observations: Grain 1 is suggested to deform less stably than grain 2, due to larger deviation of the initial orientation from the final ⟨1 1 0⟩-texture. There is a greater tendency in grain 1 to develop regions deforming on a different set of slip systems. In between those regions permanent subgrain boundaries develop which continuously increase in misorientation. The frequency of occurrence of such intermediate and large angle boundaries is much higher in grain 1 compared to grain 2. The difference in the amount of permanent boundaries with relatively large misorientations persists throughout recovery leading to subgrain growth. Thus the subgrains in grain 1 will have more misoriented boundaries than in grain 2. As boundaries with large misorientation and high mobility are a necessary condition for a subgrain to act as a nucleus of a recrystallized grain, nucleation is facilitated in grain 1 compared to grain 2. In addition, the driving force provided by the subgrain structure surrounding the nucleus is larger in grain 1 due to its larger amount of boundaries with larger misorientation and high specific energy. This explains why grain 1 recrystallizes much more readily than grain 2.

In conclusion, the present results support the view that grains with orientation favoring subdivision into strongly misoriented regions recrystallize more easily. These differences explain the inhomogeneous recrystallization behavior found in this material.

5. Conclusion

Grain orientation effects were observed during recrystallization of coarse-grained tantalum deformed by cold swaging. Strong differences in terms of the misorientations were observed in two neighboring grains. The grain with the larger fraction of high angle boundaries recrystallized readily. In contrast, recrystallization was absent in the other grain which can be explained by the predominance of boundaries with low angle character.

Acknowledgements

H.R.Z. Sandim is grateful to CNPq for his post-doctoral scholarship under Grant No. 200.530/98-4 (NV), to FINEP/PADCT (Project ENPM-460) for supplying the tantalum bars, and to MSc. M.F. Hupalo for his valuable assistance. He also acknowledges the University of Wales Swansea for providing the EBSD facilities.

References

[1] Köck W, Paschen P. Tantalum – processing, properties and applications. J Met 1989;41:33–9.
[2] Hughes DA, Hansen N. High angle boundaries formed by grain subdivision mechanisms. Acta Mater 1997;45:3871–86.
[3] Sandim HRZ, McQueen HJ, Blum W. Microstructure of cold swaged tantalum at large strains. Scripta Mater 2000;42:151–6.
[4] Hupalo MF. Dissertation. FAENQUIL, Lorena, Brazil, 1999.
[5] Theyssier MC, Chenal B, Driver JH, Hansen N. Mosaic dislocation structures in aluminium crystals deformed in multiple slip at 0.5–0.8T_M. Phys Stat Sol A 1995;149:367–78.
[6] Hjelen J, Ørsund R, Nes E. On the origin of recrystallization textures in aluminium. Acta Metall Mater 1991;39:1377–404.
[7] Furu T, Marthinsen K, Nes E. Modelling recrystallisation. Mater Sci Technol 1990;6:1093–102.
[8] Raabe D. Investigation of the orientation dependence of recovery in low-carbon steel by use of single orientation determination. Steel Res 1995;66:222–9.
[9] Raabe D, Roters F, Marx V. Experimental investigation and numerical simulation of the correlation of recovery and texture in bcc metals and alloys. Textures Microstruct 1996;26–27:611–35.
[10] Vandermeer Jr. RA, Snyder WB. Recovery and recrystallization in rolled tantalum single crystals. Metall Trans A 1979;10: 1031–44.